


Wave Packet Spreading with Disordered Nonlinear Discrete-Time Quantum Walks

Ihor Vakulchyk,^{1,2} Mikhail V. Fistul,^{1,3} and Sergej Flach¹

¹Center for Theoretical Physics of Complex Systems, Institute for Basic Science(IBS), Daejeon, Korea, 34126

²Basic Science Program, Korea University of Science and Technology (UST), Daejeon, Korea, 34113

³Russian Quantum Center, National University of Science and Technology “MISIS”, 119049 Moscow, Russia

 (Received 15 June 2018; published 30 January 2019)

We use a novel unitary map toolbox—discrete-time quantum walks originally designed for quantum computing—to implement ultrafast computer simulations of extremely slow dynamics in a nonlinear and disordered medium. Previous reports on wave packet spreading in Gross-Pitaevskii lattices observed subdiffusion with the second moment $m_2 \sim t^{1/3}$ (with time in units of a characteristic scale t_0) up to the largest computed times of the order of 10^8 . A fundamental and controversially debated question—whether this process can continue *ad infinitum*, or has to slow down—stands unresolved. Current experimental devices are not capable to even reach $1/10^4$ of the reported computational horizons. With our toolbox, we outperform previous computational results and observe that the universal subdiffusion persists over an additional four decades reaching “astronomic” times 2×10^{12} . Such a dramatic extension of previous computational horizons suggests that subdiffusion is universal, and that the toolbox can be efficiently used to assess other hard computational many-body problems.

DOI: [10.1103/PhysRevLett.122.040501](https://doi.org/10.1103/PhysRevLett.122.040501)

Eigenstates of linear excitations in a one-dimensional medium exposed to an uncorrelated random external field are exponentially localized in space, due to the celebrated Anderson localization (AL) [1]. Thus any evolving compact wave packet in such a system will first spread, but then halt and not escape from its localization volume. The width of the wave packet will be of the order of the localization length ξ [2]. Experimental verifications of AL with Bose-Einstein condensates of ultracold atomic gases loaded onto optical potentials were using precisely the above technique, i.e., the time evolution of a wave packet, to prove and quantitatively characterize the degree of AL [3,4]. Numerous further experimental studies of AL employ light [5,6], microwaves [7], and ultrasound [8,9], among others (see also Ref. [10] for a recent review).

The interplay of disorder with many body interactions intrigued the minds of researchers ever since AL was established. Recent experimental attempts include granular chains [11], photonic waveguide lattices [6], light propagation in fiber arrays [12], and atomic Bose-Einstein condensates [13]. In particular, the latter case studying the spatial extension of clouds of interacting ^{39}K atoms revealed the destruction of AL through the onset of subdiffusion—an extremely slow process of wave packet spreading with its second moment $m_2 \sim t^\alpha$ with $\alpha < 1$. Here time t is measured in units of a characteristic microscopic timescale t_0 . For example, for ultracold atomic gases this timescale $t_0 \simeq 1$ ms [13]. Different values of the exponent α were measured, which ranged between 0.1 and 0.5. That imprecision is due to the slow dynamics of subdiffusion that did not allow us to quantitatively assess

the subdiffusion exponents. For example, in the atomic gas case, the need to keep the condensate coherent, results in a time limitation of about 10^4 , i.e., about 10 s. Thus there is a clear need for alternative computational studies which may shed light on the fate of expanding wave packets. With the large number ($\sim 10^6$) of interacting cold atoms, semiclassical approximations lead to effective nonlinear wave equations similar to the celebrated Gross-Pitaevskii one, with two-body interactions turning into quartic anharmonicity.

Computational studies of spreading wave packets in various nonlinear and disordered systems revealed intriguing features. On times up to 10^2 , an initially compact wave packet expands up to the size of localization length ξ . After that a subdiffusive spreading of the wave packet [14,15] with $\alpha \approx 1/3$ occurs. At large times the wave packet is composed of a still growing central flat region of size $m_2^{1/2} \gg \xi$ with sharp boundaries of size ξ .

Qualitatively the subdiffusion can be explained as follows. The chaotic dynamics inside the wave packet leads to dephasing of the participating localized Anderson normal modes. With coherence lost, wave localization cannot be sustained anymore. The assumption of strong chaos (quick and complete dephasing of *all* modes) results in the stochastic interaction between the localized normal modes and the prediction $\alpha = 1/2$ [15]. An additional unproven phenomenological estimate of the impact of finite but small probabilities of resonances between interacting normal modes finally leads to a substantial suppression of dephasing and the correct value $\alpha = 1/3$ [15]. Interestingly, the validity of this estimate was confirmed with tests of its

predictions for larger system dimensions [16], and different exponents of nonlinear terms, which correspond to various N -body interactions [17]. Successful tests of systems with quasiperiodic (instead of random) potentials [18], and nonlinear versions of quantum kicked rotors [19,20] yielded subdiffusion with $\alpha = 1/3$ as well, and revealed additional universality aspects of the observed process [10]. The largest times reached by these computations were 10^8 – 10^9 . In the case of one single disorder realization, a reported evolution for a Klein-Gordon chain reached time 10^{10} [21]. As a side note, in weakly nonlinear systems Anderson localization in the evolution of finite size wave packets is restored in a probabilistic manner [22–24].

Remarkably, a number of published arguments predict exactly the opposite outcome—that the spreading has to slow down [22,25–28], perhaps from a subdiffusive down to a logarithmic one [29]. These arguments use perturbation approaches which might (or might not) be of little help when chaotic dynamics hits. Various attempts to observe a slow down were not successful but also limited by the computational horizons. This calls for a new approach, which can move the horizons considerably.

To address the fundamental question of whether wave packet spreading slows down or continues, we use a novel unitary map toolbox—discrete-time quantum walks (DTQW). Their highly efficient coding implementation is the key to address suitable hard computational problems with Hamiltonian dynamics and to extend beyond Hamiltonian computational limits. We peek beyond previous horizons set by the CPU time limits for systems of coupled ordinary differential equations. We obtain results for unprecedented times up to 2×10^{12} and thereby shift the old Gross-Pitaevskii horizons by four decades.

DTQW were introduced as quantum generalizations of classical random walks by Aharonov *et al.* [30]. The DTQW evolution is a (discrete) sequence of unitary operators acting on a quantum state in a high dimensional Hilbert space. DTQW shows quantum interference or superposition [30], entanglement [31], two-body coupling of wave functions [32], Anderson localization [33], etc. DTQW experimental realizations were reported with ion trap systems [34], quantum optical waveguides [35], and nuclear magnetic resonance quantum computer [36]. Quantum walks are studied by the quantum computing community since they allow for implementing algorithms which exponentially surpass known classical ones [37,38].

Consider a single quantum particle with an internal spin degree of freedom, moving on a one-dimensional lattice. Its dynamics is determined by a time- and lattice-site-dependent two-component wave function $\Psi_n(t) = \{\Psi_n^+, \Psi_n^-\}$, which evolves under the influence of some periodic Floquet drive. Then, its evolution can be mapped on to a sequence of unitary maps. The unitary map evolves the wave function over one period of the unspecified Floquet drive. For a DTQW, this map is the product of a *coin*

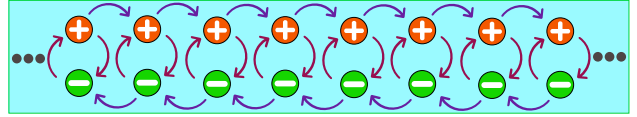


FIG. 1. A schematic representation of a general discrete-time quantum walk. The vertical arrows indicate the quantum coin action within each two level system, while the horizontal ones show the action of the transfer operator.

operator \hat{S} and a *transfer* operator \hat{T}_\pm . The coin operator $\hat{S} = \sum_n \hat{S}_n = \sum_n \hat{V}_n |n\rangle\langle n|$, with the single site quantum coin

$$\hat{V}_n = \begin{pmatrix} \cos \theta & e^{i\varphi_n} \sin \theta \\ -e^{-i\varphi_n} \sin \theta & \cos \theta \end{pmatrix}. \quad (1)$$

A schematic map flow is shown in Fig. 1. This unitary matrix parametrization is a particular realization of the general case discussed in Ref. [39], with two angles θ (kinetic energy) and φ_n (site dependent internal synthetic flux). Such coin operators can be implemented by time-dependent perturbations [40–43].

The transfer operator

$$\hat{T}_\pm = \sum_n |n\rangle\langle n+1| \otimes |\mp\rangle\langle \mp| + |n\rangle\langle n-1| \otimes |\pm\rangle\langle \pm|, \quad (2)$$

with \pm corresponding to the $+$ components shifting either to the right or to the left. We will use T_+ across the Letter. The DTQW evolution follows as a sequence of successive \hat{S} and \hat{T}_+ operators acting on the state:

$$\Psi_n(t+1) = \hat{M}_{n-1,+} \Psi_{n-1}(t) + \hat{M}_{n+1,-} \Psi_{n+1}(t), \quad (3)$$

where the matrices $\hat{M}_{n,\pm}$ are defined by the elements of \hat{V}_n :

$$\hat{M}_+ = \begin{pmatrix} V_{11} & V_{12} \\ 0 & 0 \end{pmatrix}, \quad \hat{M}_- = \begin{pmatrix} 0 & 0 \\ V_{21} & V_{22} \end{pmatrix}. \quad (4)$$

Next, we consider a strongly disordered DTQW with random uncorrelated angles φ_n being uniformly distributed over the entire existence domain $[-\pi, \pi)$. The resulting unitary eigenvalue problem is solved by finding the orthonormal set of eigenvectors $\{\tilde{\Psi}_{\nu,n}\}$ with $\tilde{\Psi}_{\nu,n}(t+1) = e^{-i\omega_\nu} \tilde{\Psi}_{\nu,n}(t)$ and the eigenvalues $e^{-i\omega_\nu}$, where ω_ν is the quasienergy. All eigenvectors are exponentially localized on the chain [39]. This is a manifestation of Anderson localization. Remarkably, for such strong disorder all eigenvectors $\tilde{\Psi}_{\nu,|n| \rightarrow \infty} \sim e^{-|n|/\xi}$ are characterized by one single localization length $\xi(\theta)$ which *does not* depend on the quasienergy ω_ν of a given state [39]:

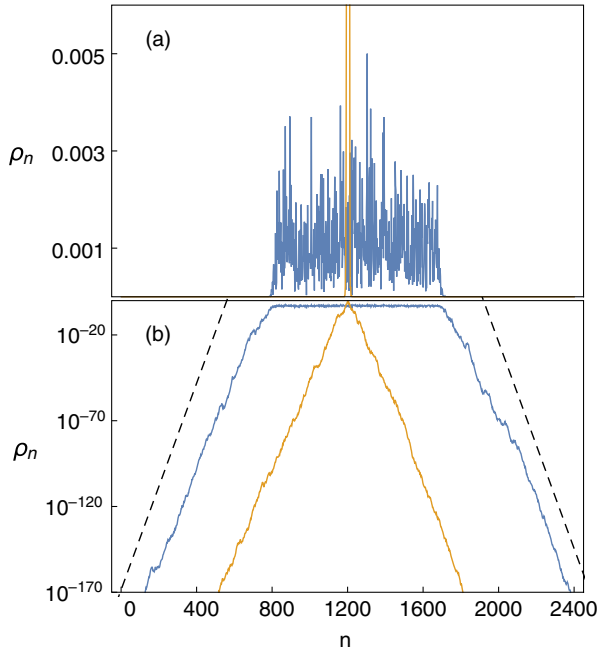


FIG. 2. Wave packet density profiles ρ_n for linear $g = 0$ (orange solid lines) and nonlinear $g = 3$ (blue solid lines) DTQWs at the time $t_f = 10^8$ (linear case) and $t_f = 2 \times 10^{12}$ (nonlinear case). (a) lin-lin plot. (b) log-normal plot. The black dashed lines indicate exponential decay with the corresponding localization length $e^{-2|n-n_0|/\xi}$.

$$\xi = -\frac{1}{\ln(|\cos(\theta)|)}. \quad (5)$$

Another remarkable feature is that for any value of the localization length—either small or large compared to the lattice spacing $\Delta n \equiv 1$ —the spectrum of the quasienergies of an infinite chain is densely filling the compact space of angles of complex numbers on a unit circle [39]. Therefore, the density of states is constant, and gaps in the spectrum are absent.

Anderson localization is manifested through the halt of spreading of an evolving wave packet. In our direct numerical simulations, we choose $\theta = \pi/4$, which results in a localization length $\xi \approx 2.9$ and a typical localized Anderson eigenstate occupying about 10 lattice sites. We choose the initial state to be localized on M sites:

$$\Psi_n(t=0) = \frac{1}{\sqrt{2M}}(1, i), \quad n = n_0, \dots, (n_0 + M - 1). \quad (6)$$

We evolve this state using Eq. (3) until $t = 10^8$ for a system of size $N = 2400$ and $M = 1$. The density distribution $\rho_n(t) = |\Psi_n^-|^2 + |\Psi_n^+|^2$ observed for such time is presented in Fig. 2(a) (orange solid lines). The distribution is clearly localized, with the width of a few localization lengths. The tails are exponentially decaying, with a slope which is well fitted using the localization length ξ in Fig. 2(b). To further

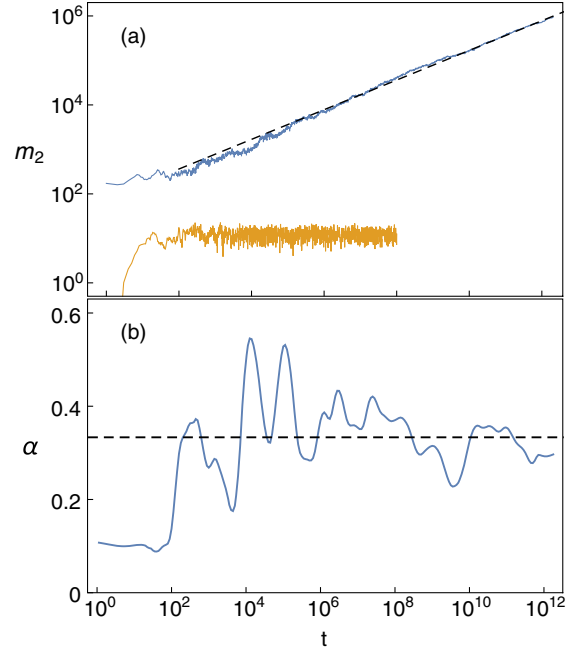


FIG. 3. (a) $m_2(t)$ versus time in log-log scale for the linear $g = 0$ (orange solid lines) and nonlinear $g = 3$ (blue solid lines) case from Fig. 2. (b) The derivative $\alpha(t)$ versus time for the data of the nonlinear run from (a) (blue line). Black dashed line corresponds to $\alpha = 1/3$.

quantify the halt of spreading, we compute the first moment $\bar{n}(t) = \sum_{n=1}^N n \rho_n(t)$, and then the central object of our studies—the second moment

$$m_2(t) = \sum_{n=1}^N [n - \bar{n}(t)]^2 \rho_n(t). \quad (7)$$

The time dependence of m_2 is plotted in Fig. 3(a). We observe a halt of the growth of $m_2(t)$ at $t \approx 10^2$, which together with the profile of the halted wave packet (see Fig. 2) is a clear demonstration of Anderson localization.

We now leave the grounds of linear DTQW and generalize the DTQW to a *nonlinear* unitary map by adding a density-dependent renormalization to the angle

$$\varphi_n = \xi_n + g\rho_n, \quad (8)$$

where g is the nonlinearity strength. We note that Eq. (8) keeps the conservation of the total norm: $\sum_n \dot{\rho}_n = 0$.

Our main goal is to measure the details of subdiffusive wave packet spreading on large timescales with $\rho_n \ll 1$. Therefore, we use a low-density approximation for the quantum coin (1) which approximates the exponential factors of the coin without violating evolution unitarity:

$$e^{i\varphi_n} = e^{i\xi_n} \left(\sqrt{1 - g^2 \rho_n^2} + ig\rho_n \right). \quad (9)$$

The computational advantage of fast calculations of square roots as opposed to slow ones of trigonometric functions serves the purpose to further extend the simulation times. To guarantee unitarity of the evolution, we choose $M > 1$ such that $g^2 \rho_n^2 \ll 1$.

We evolve a wave packet with $g = 3$ and $M = 13$ and plot the density distribution at the final time $t_f = 2 \times 10^{12}$ in Fig. 2 (blue solid line). This is a new record evolution time, beating old horizons by a factor of 10^4 . We observe a familiar structure of the wave packet: a homogeneous wide central part with clean remnants of Anderson localization in the tails [Fig. 2(b)]. The width of the wave packet reaches about 900 sites and exceeds the localization length ξ by a stunning factor of about 300. The time dependence of the second moment $m_2(t)$ is plotted in Fig. 3(a). A clean and steady growth of the wave packet width is evident, and the linear fitting on the log-log scale [black line in Fig. 3(a)] indicates the universal $\alpha = 1/3$ value.

However, we note that a straightforward fitting with a single power law can yield misleading results, since it is not evident where the asymptotic regime (if any) will start. To study the asymptotic regime in detail we quantitatively assess it by applying standard methods of simulations and data analysis [44]. We calculate local derivatives on log-log scales to obtain a time-dependent exponent $\alpha(t) = d[\ln(m_2)]/d[\ln t]$. The resulting curve is plotted in Fig. 3(b) and strongly fluctuates around the value $1/3$.

In order to reduce the fluctuation amplitudes, we obtain $m_{2,n}(t)$ for $R = 108$ disorder realizations and compute the geometric average $\ln \bar{m}_2(t) = \sum_n \ln m_{2,n}(t)/R$. In Fig. 4(a) the results are shown for various values of $g = 0.5, 1, 1.5, 2, 2.5$ up to times 10^8 (the corresponding values of M are 5,8,8,10,10). All curves approach the vicinity of $\alpha = 1/3$

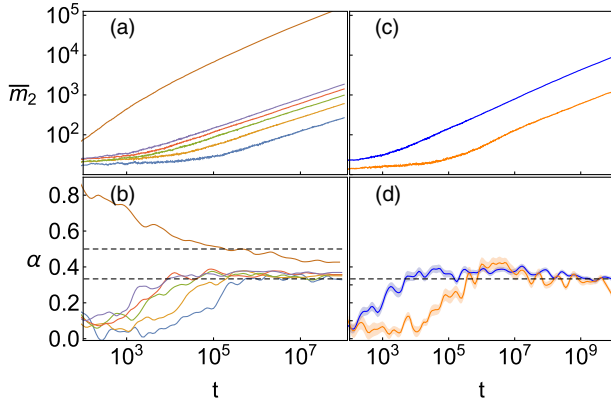


FIG. 4. (a) The geometric average \bar{m}_2 versus time for 108 disorder realizations up to time $t = 10^8$. The nonlinear parameter g varies from bottom to top as 0.5 (blue), 1 (orange), 1.5 (green), 2 (red), 2.5 (purple), and 50 (brown). (b) The derivative $\alpha(t)$ versus time for the data from (a) and same color codes. The horizontal dashed line corresponds to $\alpha = 1/3$. (c),(d) Same as in (a),(b) but for $g = 2.5$ (blue) and $g = 0.5$ (orange) and up to time $t = 10^{10}$. Shaded areas indicate the statistical error.

with fluctuation amplitudes substantially reduced as compared to the single run in Fig. 3(b). For $g = 0.5$ and $g = 2.5$ we extend the simulations up to time 10^{10} in Fig. 4(c) and observe a clear saturation of $\alpha(t)$ around $1/3$ in Fig. 4(d). In particular, the weakest nonlinearity value $g = 0.5$ is expected to show the earliest onset of asymptotic subdiffusion. Indeed we find in this case $\alpha = 1/3 \pm 0.04$ starting with times $t \geq 10^7$.

For $g = 50$ we obtain a speedup of subdiffusion with $\alpha(t) > 1/3$, which then slowly converges to the asymptotic one with $\alpha = 1/3$ (Fig. 4). We thus observe a crossover from weak to strong chaos similar to Ref. [48]. We have not observed any slowing down beyond the $\alpha = 1/3$ law in the whole range of newly accessible times.

It is instructive to rewrite the evolution equations in the basis of linear eigenmodes of the $g = 0$ case. Using the Taylor expansion of nonlinear terms valid at large times when $\rho_n \ll 1$ [44] we rewrite the unitary evolution of the wave function in the $g = 0$ eigenmode basis $\Psi_n(t) = \sum_\alpha a_\alpha(t) \tilde{\Psi}_{\alpha,n}$:

$$a_\alpha(t+1) = a_\alpha(t) e^{i\omega_\alpha} + ig \sin \theta \sum_{\alpha_1, \alpha_2, \alpha_3}^{2N} I_{\alpha, \alpha_1, \alpha_2, \alpha_3} a_{\alpha_1}(t)^* a_{\alpha_2}(t) a_{\alpha_3}(t), \quad (10)$$

with the overlap integral

$$I_{\alpha, \alpha_1, \alpha_2, \alpha_3} = \sum_{k=1}^N \langle \tilde{\Psi}_{\alpha, k} | \hat{u}^{(k)} \tilde{\Psi}_{\alpha_3, k} \rangle \langle \tilde{\Psi}_{\alpha_1, k} | \tilde{\Psi}_{\alpha_2, k} \rangle. \quad (11)$$

The structure of these resulting equations is strikingly similar to the ones obtained from Hamiltonian dynamics [14,15]. In particular, we obtain cubic nonlinear terms on the right-hand side of the asymptotic expansion (10). Together with the one dimensionality of the system the prediction of a subdiffusive exponent $\alpha = 1/3$ follows from Refs. [14,15].

To conclude, DTQW are very useful unitary map toolboxes which allow for extremely fast quantum evolution, in particular due to covering finite times with one step (jump), and due to the fast(est) realization of a transfer, hopping, or interaction on a lattice. We used a disordered version to obtain Anderson localization with the spectrum being dense and gapless and of compact support. The resulting localization length ξ is not depending on the eigenvalue of an eigenstate and can be smoothly changed in its whole range of existence using one of the control parameters of the DTQW. All these features induce highest aesthetical satisfaction for what is to come. We then generalize the map to a nonlinear disordered DTQW and study destruction of Anderson localization. Wave packets spread subdiffusively with their second moment $m_2 \sim t^\alpha$ and the universal exponent $\alpha = 1/3$. The record time $t_f = 2 \times 10^{12}$

is reached, which exceeds old horizons by 3–4 orders of magnitude. The size of the wave packet reaches $\approx 300\xi$. The relative strength (or better weakness) of the nonlinear terms in the DTQW reaches $0.01/\pi \approx 0.003$. No slowing down of the subdiffusive process was observed. Therefore chaotic dynamics appears to survive in the asymptotic limit of decreasing wave packet densities.

We expect DTQW to be useful in the future also for exploring other hard computational tasks, e.g., subdiffusion in two-dimensional and even three-dimensional nonlinear disordered lattices, and many body localization in interacting quantum settings.

This work was supported by the Institute for Basic Science, Project Code (IBS-R024-D1).

-
- [1] P. W. Anderson, Absence of diffusion in certain random lattices, *Phys. Rev.* **109**, 1492 (1958).
- [2] I. M. Lifshits, S. A. Gredeskul, and L. A. Pastur, *Introduction to the Theory of Disordered Systems* (Wiley-Interscience, New York, 1988).
- [3] J. Billy, V. Josse, Z. Zuo, A. Bernard, B. Hambrecht, P. Lugan, D. Clément, L. Sanchez-Palencia, P. Bouyer, and A. Aspect, Direct observation of Anderson localization of matter waves in a controlled disorder, *Nature (London)* **453**, 891 (2008).
- [4] G. Roati, C. D’Errico, L. Fallani, M. Fattori, C. Fort, M. Zaccanti, G. Modugno, M. Modugno, and M. Inguscio, Anderson localization of a non-interacting Bose-Einstein condensate, *Nature (London)* **453**, 895 (2008).
- [5] T. Schwartz, G. Bartal, S. Fishman, and M. Segev, Transport and Anderson localization in disordered two-dimensional photonic lattices, *Nature (London)* **446**, 52 (2007).
- [6] Y. Lahini, A. Avidan, F. Pozzi, M. Sorel, R. Morandotti, D. N. Christodoulides, and Y. Silberberg, Anderson Localization and Nonlinearity in One-Dimensional Disordered Photonic Lattices, *Phys. Rev. Lett.* **100**, 013906 (2008).
- [7] R. Dalichaouch, J. P. Armstrong, S. Schultz, P. M. Platzman, and S. L. McCall, Microwave localization by two-dimensional random scattering, *Nature (London)* **354**, 53 (1991).
- [8] R. L. Weaver, Anderson localization of ultrasound, *Wave Motion* **12**, 129 (1990).
- [9] H. Hu, A. Strybulevych, J. H. Page, S. E. Skipetrov, and B. A. van Tiggelen, Localization of ultrasound in a three-dimensional elastic network, *Nat. Phys.* **4**, 945 (2008).
- [10] T. V. Lapyeva, M. V. Ivanchenko, and S. Flach, Nonlinear lattice waves in heterogeneous media, *J. Phys. A* **47**, 493001 (2014).
- [11] E. Kim, A. J. Martínez, S. E. Phenisee, P. G. Kevrekidis, M. A. Porter, and J. Yang, Direct measurement of superdiffusive energy transport in disordered granular chains, *Nat. Commun.* **9**, 640 (2018).
- [12] T. Pertsch, U. Peschel, J. Kobelke, K. Schuster, H. Bartelt, S. Nolte, A. Tünnermann, and F. Lederer, Nonlinearity and Disorder in Fiber Arrays, *Phys. Rev. Lett.* **93**, 053901 (2004).
- [13] E. Lucioni, B. Deissler, L. Tanzi, G. Roati, M. Zaccanti, M. Modugno, M. Larcher, F. Dalfovo, M. Inguscio, and G. Modugno, Observation of Subdiffusion in a Disordered Interacting System, *Phys. Rev. Lett.* **106**, 230403 (2011).
- [14] A. S. Pikovsky and D. L. Shepelyansky, Destruction of Anderson Localization by a Weak Nonlinearity, *Phys. Rev. Lett.* **100**, 094101 (2008).
- [15] S. Flach, D. O. Krimer, and Ch Skokos, Universal Spreading of Wave Packets in Disordered Nonlinear Systems, *Phys. Rev. Lett.* **102**, 024101 (2009).
- [16] T. V. Lapyeva, J. D. Bodyfelt, and S. Flach, Subdiffusion of nonlinear waves in two-dimensional disordered lattices, *Europhys. Lett.* **98**, 60002 (2012).
- [17] Ch. Skokos and S. Flach, Spreading of wave packets in disordered systems with tunable nonlinearity, *Phys. Rev. E* **82**, 016208 (2010).
- [18] M. Larcher, T. V. Lapyeva, J. D. Bodyfelt, F. Dalfovo, M. Modugno, and S. Flach, Subdiffusion of nonlinear waves in quasiperiodic potentials, *New J. Phys.* **14**, 103036 (2012).
- [19] D. L. Shepelyansky, Delocalization of Quantum Chaos by Weak Nonlinearity, *Phys. Rev. Lett.* **70**, 1787 (1993).
- [20] G. Gligorić, J. D. Bodyfelt, and S. Flach, Interactions destroy dynamical localization with strong and weak chaos, *Europhys. Lett.* **96**, 30004 (2011).
- [21] Ch. Skokos, D. O. Krimer, S. Komineas, and S. Flach, Delocalization of wave packets in disordered nonlinear chains, *Phys. Rev. E* **79**, 056211 (2009).
- [22] M. Johansson, G. Kopidakis, and S. Aubry, Kam tori in 1D random discrete nonlinear Schrödinger model?, *Europhys. Lett.* **91**, 50001 (2010).
- [23] M. V. Ivanchenko, T. V. Lapyeva, and S. Flach, Anderson Localization or Nonlinear Waves: A Matter of Probability, *Phys. Rev. Lett.* **107**, 240602 (2011).
- [24] D. M. Basko, Weak chaos in the disordered nonlinear Schrödinger chain: Destruction of Anderson localization by Arnold diffusion, *Ann. Phys. (Amsterdam)* **326**, 1577 (2011).
- [25] S. Fishman, Y. Krivolapov, and A. Soffer, The nonlinear Schrödinger equation with a random potential: Results and puzzles, *Nonlinearity* **25**, R53 (2012).
- [26] D. M. Basko, Kinetic theory of nonlinear diffusion in a weakly disordered nonlinear Schrödinger chain in the regime of homogeneous chaos, *Phys. Rev. E* **89**, 022921 (2014).
- [27] F. Huveneers, Drastic fall-off of the thermal conductivity for disordered lattices in the limit of weak anharmonic interactions, *Nonlinearity* **26**, 837 (2013).
- [28] D. M. Basko, Local nature and scaling of chaos in weakly nonlinear disordered chains, *Phys. Rev. E* **86**, 036202 (2012).
- [29] W. De Roeck and F. Huveneers, Asymptotic localization of energy in nondisordered oscillator chains, *Commun. Pure Appl. Math.* **68**, 1532 (2015).
- [30] Y. Aharonov, L. Davidovich, and N. Zagury, Quantum random walks, *Phys. Rev. A* **48**, 1687 (1993).
- [31] G. Abal, R. Siri, A. Romanelli, and R. Donangelo, Quantum walk on the line: Entanglement and nonlocal initial conditions, *Phys. Rev. A* **73**, 042302 (2006).

- [32] Y. Omar, N. Paunković, L. Sheridan, and S. Bose, Quantum walk on a line with two entangled particles, *Phys. Rev. A* **74**, 042304 (2006).
- [33] A. Crespi, R. Osellame, R. Ramponi, V. Giovannetti, R. Fazio, L. Sansoni, F. De Nicola, F. Sciarrino, and P. Mataloni, Anderson localization of entangled photons in an integrated quantum walk, *Nat. Photonics* **7**, 322 (2013).
- [34] H. Schmitz, R. Matjeschk, Ch Schneider, J. Glueckert, M. Enderlein, T. Huber, and T. Schaetz, Quantum Walk of a Trapped Ion in Phase Space, *Phys. Rev. Lett.* **103**, 090504 (2009).
- [35] A. Peruzzo, M. Lobino, J. C. F. Matthews, N. Matsuda, A. Politi, K. Poulios, X.-Q. Zhou, Y. Lahini, N. Ismail, K. Wörhoff *et al.*, Quantum walks of correlated photons, *Science* **329**, 1500 (2010).
- [36] J. Du, H. Li, X. Xu, M. Shi, J. Wu, X. Zhou, and R. Han, Experimental implementation of the quantum random-walk algorithm, *Phys. Rev. A* **67**, 042316 (2003).
- [37] A. M. Childs, R. Cleve, E. Deotto, E. Farhi, S. Gutmann, and D. A. Spielman, Exponential algorithmic speedup by a quantum walk, in *Proceedings of the Thirty-fifth Annual ACM Symposium on Theory of Computing, STOC '03* (ACM, New York, 2003), pp. 59–68.
- [38] E. Farhi, J. Goldstone, and S. Gutmann, A quantum algorithm for the Hamiltonian NAND tree, *Theory Comput.* **4**, 169 (2008).
- [39] I. Vakulchyk, M. V. Fistul, P. Qin, and S. Flach, Anderson localization in generalized discrete-time quantum walks, *Phys. Rev. B* **96**, 144204 (2017).
- [40] Y. Makhlin, G. Schön, and A. Shnirman, Quantum-state engineering with Josephson-junction devices, *Rev. Mod. Phys.* **73**, 357 (2001).
- [41] B. C. Sanders, S. D. Bartlett, B. Tregenna, and P. L. Knight, Quantum quincunx in cavity quantum electrodynamics, *Phys. Rev. A* **67**, 042305 (2003).
- [42] T. Di, M. Hillery, and M. S. Zubairy, Cavity qed-based quantum walk, *Phys. Rev. A* **70**, 032304 (2004).
- [43] M. Karski, L. Förster, J.-M. Choi, A. Steffen, W. Alt, D. Meschede, and A. Widera, Quantum walk in position space with single optically trapped atoms, *Science* **325**, 174 (2009).
- [44] See Supplemental Material at <http://link.aps.org/supplemental/10.1103/PhysRevLett.122.040501> for a brief description of the derivation of the asymptotic evolution equation and the numerical approach, which includes Refs. [45–47].
- [45] W. S. Cleveland, Lowess: A program for smoothing scatterplots by robust locally weighted regression, *American Statistician* **35**, 54 (1981).
- [46] W. S. Cleveland and S. J. Devlin, Locally weighted regression: An approach to regression analysis by local fitting, *J. Am. Stat. Assoc.* **83**, 596 (1988).
- [47] R. J. Hodrick and E. C. Prescott, Postwar U.S. business cycles: An empirical investigation, *J. Money, Credit Banking* **29**, 1 (1997).
- [48] T. V. Lapyteva, J. D. Bodyfelt, D. O. Krimer, Ch. Skokos, and S. Flach, The crossover from strong to weak chaos for nonlinear waves in disordered systems, *Europhys. Lett.* **91**, 30001 (2010).